Recombinant Thrombomodulin Domain 1 Modulates Macrophage Polarization and Enhances Healing in Corneal Alkali Burns

Chun-Hsiang Chang, I-Chen Peng, and Yi-Hsun Huang

Department of Ophthalmology, National Cheng Kung University Hospital, College of Medicine, National Cheng Kung University, Tainan, Taiwan

Correspondence: Yi-Hsun Huang, Department of Ophthalmology, National Cheng Kung University Hospital, College of Medicine, National Cheng Kung University, 138 Sheng-Li Rd., Tainan 704, Taiwan; jackhyh@gmail.com.

Received: October 25, 2024
Accepted: December 14, 2024
Published: January 9, 2025

Citation: Chang CH, Peng IC, Huang YH. Recombinant thrombomodulin domain 1 modulates macrophage polarization and enhances healing in corneal alkali burns. *Invest Ophthalmol Vis Sci.* 2025;66(1):21. https://doi.org/10.1167/iovs.66.1.21

Purpose. Corneal alkali burns are severe ocular injuries characterized by intense inflammation, tissue damage, and vision impairment, with current treatments often insufficient in restoring corneal function and clarity. This study aimed to evaluate the therapeutic effects of recombinant thrombomodulin domain 1 (rTMD1) in the treatment of corneal alkali burns, focusing on its impact on inflammation, tissue repair, fibrosis, and neovascularization.

Methods. A murine model of corneal alkali burn was utilized to investigate the therapeutic potential of rTMD1. The effects of rTMD1 on macrophage polarization, inflammatory response, tissue repair, fibrosis, and neovascularization were assessed through histological analysis, immunohistochemistry, and molecular studies targeting key signaling pathways such as ERK/HIF-1α and vascular endothelial growth factor (VEGF) expression.

Results. Administration of rTMD1 significantly modulated macrophage polarization, promoting a transition from the pro-inflammatory M1 phenotype to the reparative M2 phenotype via inhibition of the ERK/HIF-1α pathway. This shift resulted in reduced inflammation, enhanced tissue repair, and controlled fibrosis. Furthermore, rTMD1 inhibited neovascularization by downregulating VEGF expression, aiding in the preservation of corneal clarity.

Conclusions. rTMD1 demonstrates substantial therapeutic potential in treating corneal alkali burns by reducing inflammation, promoting tissue repair, controlling fibrosis, and inhibiting neovascularization. These findings support the further development of rTMD1 as a promising treatment for corneal burns and possibly other inflammatory ocular conditions.

Keywords: anti-inflammatory, corneal alkali burn, corneal neovascularization, macrophage polarization, recombinant thrombomodulin domain 1 (rTMD1)

Chemical burns of the ocular surface are major ophthalmic emergencies that require immediate treatment. The incidence rate of ocular chemical burns ranges from 11.5% to 22.1% of all ocular traumas, with most accidents occurring in the workplace.[1] Alkali solutions, commonly found in cleaning products, cause more injuries than acid solutions due to their higher lipid solubility and greater tissue penetration, resulting in more severe damage to the cornea.[2–4] Corneal neovascularization and fibrosis are common outcomes of alkali burns, eventually leading to opacity and visual impairment.[1,2,5] Additionally, persistent loss of marginal corneal arcades and alterations in the limbal microvasculature have been identified as critical prognostic factors, with techniques such as fluorescein and indocyanine green angiography providing objective assessments over time.[6] Therefore, maintaining corneal transparency is crucial for a favorable outcome.

Thrombomodulin (TM) is a transmembrane glycoprotein originally identified in vascular endothelium.[7] It consists of five domains: a highly charged N-terminal lectin-like domain (D1), a domain with six epidermal growth factor–like structures (D2), a serine- and threonine-rich domain (D3), a transmembrane domain (D4), and a cytoplasmic domain (D5).[8,9] Different domains of TM have distinct functions, and the anti-angiogenic and anti-inflammatory effects of the recombinant lectin-like domain of TM have already been demonstrated.[10,11]

Upon injury, macrophages infiltrate the cornea and play a pivotal role in the ensuing inflammatory and healing processes through their polarization into M1 and M2 phenotypes.[12] M1 macrophages, activated by pro-inflammatory signals, produce high levels of cytokines and reactive species that exacerbate inflammation and tissue damage, potentially leading to further complications such as corneal neovascularization.[13] Conversely, M2 macrophages, induced by anti-inflammatory cues, help resolve inflammation and promote tissue repair by secreting anti-inflammatory cytokines and growth factors.[14] The balance between M1 and M2 macrophage activities is critical in determining the outcome of corneal healing.[15] Excessive M1 activity can lead to chronic inflammation and scarring, whereas appropriate M2 activity aids in tissue regeneration and reduces fibrosis,

Copyright 2025 The Authors

This work is licensed under a Creative Commons Attribution-NonCommercial-NoDerivatives 4.0 International License.

Downloaded from iovs.arvojournals.org on 01/10/2025

ultimately preserving corneal transparency and function.[16] Notably, thrombomodulin has been found to regulate M1/M2 switching.[17]

Although the effects of recombinant thrombomodulin domain 1 (rTMD1) have been previously identified, its exact role in corneal chemical burns has not been determined. Therefore, in this study, we aimed to investigate whether the anti-angiogenic and anti-inflammatory effects of rTMD1 can improve the damage caused by corneal alkali burns by regulating macrophage polarization.

Materials and Methods

Preparation of rTMD1

rTMD1 expression and purification in the *Pichia pastoris* expression system were conducted as previously described.[10] Recombinant proteins were purified using nickel-chelating Sepharose columns (Amersham Pharmacia Biotech, Uppsala, Sweden) and examined by sodium dodecyl sulfate–polyacrylamide gel electrophoresis (SDS-PAGE).

Animals

Healthy female C57BL/6J mice, 6 to 8 weeks old, were purchased from the National Cheng Kung University Laboratory Animal Center in Tainan, Taiwan. $TM^{LeD/LeD}$ mice, lacking the lectin-like domain of thrombomodulin, were provided by Edward M. Conway, PhD.[18] The right eye of each mouse was used for the experiment, and the left eye remained untreated. All experiments adhered to the ARVO Statement for the Use of Animals in Ophthalmic and Vision Research and were approved by the Institutional Animal Care and Use Committee of National Cheng Kung University (approval no: 109345).

Experimental Corneal Alkali Burn Animal Model

Mice were anesthetized with an intraperitoneal injection of a Zoletil and xylazine mixture (50 mg/kg Zoletil + 5.8 mg/kg xylazine) at a dosage of 0.1 mL/20 g body weight, along with a drop of 0.5% proparacaine hydrochloride (Alcaine eye drops; Alcon, Fort Worth, TX, USA) for topical anesthesia. A 2-mm-diameter filter paper soaked with 2.5 µL of 1-M NaOH was placed on the central cornea for 30 seconds. After the filter paper was removed, the eye was thoroughly irrigated with 20 mL of Hanks' Balanced Salt Solution (HBSS). The mice were divided into two groups: One group received a temporal side subconjunctival injection of 20 µL phosphate-buffered saline (PBS), and the other group received 20 µL of rTMD1 (2 mg/mL) using a 27-gauge needle on day 1. Both groups received topical treatments of 5 µL PBS or rTMD1 (2 mg/mL) on days 4, 7, and 10. Mice treated with PBS were classified as the PBS group, and those treated with rTMD1 were classified as the rTMD1 group.

Evaluation of Corneal Epithelial Defect, Neovascularization, and Opacity

Images of mouse corneas were captured using a slit-lamp microscope (SL-D301; Topcon, Tokyo, Japan) immediately after the alkali burn and on days 4, 7, 10, and 14. Corneal epithelial defects were visualized using 0.5% fluorescein staining under cobalt blue light. Corneal neovascularization was assessed by measuring the centricity of vessels from the limbus.[19] As previously described,[20] corneal opacity was graded on a numerical scale of 0 to 4: 0 for clear cornea, 1 for slight stromal opacity, 2 for moderate stromal opacity, 3 for severe corneal opacity with visible iris, and 4 for opaque cornea with no visible iris. Images were quantified using ImageJ software (National Institutes of Health, Bethesda, MD, USA).

Table. Sequence of DNA Primers for Real-Time PCR

Gene	Sequence of Primers (5′–3′)
VEGF	F: GGCTGCTGTAACGATGAAGC
	R: TTAACTCAAGCTGCCTCGC
VEGFR1	F: GTGATCAGCTCCAGGTTTGACTT
	R: AGGAGGATGAGGGTGTCTATAGGT
TGF-β1	F: TGATACGCCTGAGTGGCTGTCT
	R: CACAAGAGCAGTGAGCGCTGAA
TNF-α	F: CTGTAGCCCACGTCGTAGC
	R: TTTGAGATCCATGCCGTTG
CD86	F: CCCCAGACCACATTCCTTGG
	R: TGTTCACTCTCTTCCCTCTCCA
CD206	F: TACTGAACCCCCACAACTGC
	R: ACCAGAGAGGAACCCATTCG
GAPDH	F: AAGAGGGATGCTGCCCTTAC
	R: CCATTTTGTCTACGGGACGA

Histology and Immunofluorescence Staining

The eye globes from the experimental mice were isolated and fixed in 4% paraformaldehyde for 24 hours, embedded in paraffin, and cut into 5-µm sections 14 days after the alkali burn. Sections were then stained with hematoxylin and eosin (H&E). For immunofluorescent staining, slides were incubated with the primary antibodies or conjugated antibodies overnight at 4°C. After rinsing with PBS with Tween (PBST), they were flatmounted on cover slides with an aqueous mounting medium (Thermo Fisher Scientific, Waltham, MA, USA). After the washing and blocking, the flat-mounted sections were incubated with the primary antibodies overnight at 4°C. The secondary antibodies were added for 1 hour at room temperature, and the nuclei were counterstained with 4′,6-diamidino-2-phenylindole (DAPI; Hoechst 33342; Molecular Probes, Eugene, OR, USA).

TUNEL Staining

TUNEL staining was performed following the manufacturer's protocols (In Situ Cell Death Detection Kit; Roche, Mannheim, Germany), and nuclei were stained with DAPI. Images were captured using a confocal microscope (Olympus IX71; Olympus, Tokyo, Japan).

Real-Time Polymerase Chain Reaction

The High Pure RNA Isolation Kit (Roche Diagnostics, Mannheim, Germany) was used to isolate RNA from mouse corneas 14 days after alkali burn. Quantitative real-time polymerase chain reaction (qRT-PCR) was performed on a StepOne Real-Time PCR System (Applied Biosystems, Foster City, CA, USA) using the PowerUp SYBR Green Master Mix (Thermo Fisher Scientific). Primers used in this study were synthesized by Integrated DNA Technologies (Coralville, IA, USA) and are listed in the Table. Transcript quantification was performed in triplicate for each sample. Results were normalized to glyceraldehyde-3-phosphate dehydrogenase (GAPDH) and reported relative to the control group using the ΔΔCT method.

Investigative Ophthalmology & Visual Science

Downloaded from iovs.arvojournals.org on 01/10/2025

Human Monocytic Cell Line Cell Differentiation and Maintenance

The THP-1 cell line was utilized to evaluate macrophage polarization following TM application. THP-1 cells, sourced from the Bioresource Collection and Research Center (Taiwan) were cultured in RPMI 1640 medium (HiMedia, Mumbai, India) supplemented with 10% fetal bovine serum (FBS; HyClone, Logan, UT, USA) and Gibco 1% penicillin–streptomycin (Thermo Fisher Scientific). M1 macrophages were generated based on a previously described protocol with slight modifications.[21] THP-1 cells were seeded at a density of 1.5×10^5 cells/mL and treated with RPMI 1640 medium containing 150-nM phorbol 12-myristate 13-acetate (PMA; Sigma-Aldrich, St. Louis, MO, USA) for 24 hours. This was followed by a 24-hour incubation in PMA-free RPMI 1640 medium to achieve the M0 stage. Subsequently, the M0 macrophages were polarized to the M1 phenotype by incubating them in RPMI 1640 medium with 20 ng/mL IFN-γ (R&D Systems, Minneapolis, MN, USA) and 100 ng/mL lipopolysaccharide (Sigma-Aldrich) for 1 day.

In Vitro Application of rTMD1 and Macrophage Polarization

M1 macrophages were induced using an M1 induction medium, with or without the addition of rTMD1 at concentrations of 10, 20, 40, and 300 nM. After 24 hours of rTMD1 treatment, RNA and protein were extracted from the cells to assess the macrophage phenotype.

Western Blot Analysis

For the western blot analysis, 10 µg of total protein was separated by 10% SDS-PAGE and transferred onto a polyvinylidene difluoride membrane. The membranes were blocked with 5% nonfat milk powder for 1 hour at room temperature. Following blocking, the membranes were incubated overnight at 4°C with specific antibodies against extracellular signal-related kinase (ERK), phospho-ERK, hypoxia-inducible factor-1α (HIF-1α), and GAPDH. After incubation with peroxidase-conjugated secondary antibodies (EMD Biosciences, San Diego, CA, USA) for 1 hour at room temperature, protein bands were visualized using enhanced chemiluminescence reagent (Millipore, Bedford, MA, USA) and captured with a Fujifilm LAS-3000 imager (Fujifilm Life Science, Cambridge, MA, USA).

Statistical Analysis

Statistical analysis was performed using Prism 9.0 (GraphPad, Boston, MA, USA). Data are expressed as mean ± SD. Statistical significance between groups was assessed using independent samples *t*-test and analysis of variance (ANOVA). $P < 0.05$ was considered statistically significant.

Results

rTMD1 Promotes Corneal Epithelial Wound Healing

Corneal epithelial defects were visualized using fluorescein stain under cobalt blue light, revealing recovery after alkali burns in both groups. The wound closure rate at specific time points was calculated as 100% minus the percentage of the denuded area relative to the initial chemical burn area. In C57BL/6J mice, rTMD1 promoted corneal epithelial healing at all time points observed under slit-lamp examination (Fig. 1A), with a significantly improved wound closure rate compared to the PBS group (Fig. 1B). To further assess the role of TMD1 in corneal wound healing, $TM^{LeD/LeD}$ mice were used. These mice showed delayed corneal epithelial wound healing compared to C57BL/6J mice (Fig. 1C). Additionally, rTMD1 significantly improved the wound healing rate at all time points compared to the PBS group (Fig. 1D).

rTMD1 Ameliorates Alkali Burn-Induced Corneal Neovascularization

The progression of corneal neovascularization (CNV) was observed following corneal alkali burns. However, in C57BL/6J mice, the number and tortuosity of vessels were significantly reduced in the rTMD1 group compared to the PBS group at all time points (Fig. 2A). CNV was evaluated by measuring the centricity (length of the longest vessel from the limbus), showing a significant decrease in vessel length in the rTMD1-treated group (Fig. 2B). In $TM^{LeD/LeD}$ mice, CNV was more severe than in C57BL/6J mice on day 14 in both the untreated and PBS-treated groups (Fig. 2C). The centricity of CNV was significantly decreased in the rTMD1-treated group (Fig. 2D).

rTMD1 Exhibits Antifibrotic, Anti-Inflammation, and Anti-Apoptosis Effects In Vivo

Corneal opacity was observed following alkali burns in both C57BL/6J and $TM^{LeD/LeD}$ mice. The corneal opacity scores were significantly lower in the rTMD1-treated group compared to the PBS group (Fig. 3A). H&E staining revealed an aggregation of inflammatory cells, as well as thickening and fibrosis of the cornea post-alkali burn, with more severe effects in $TM^{LeD/LeD}$ mice. rTMD1 treatment improved these inflammatory and fibrotic responses (Fig. 3B). Additionally, immunostaining for alpha-smooth muscle actin (α-SMA) indicated reduced fibrosis in the rTMD1 group compared to the PBS group on day 14, whereas $TM^{LeD/LeD}$ mice exhibited higher α-SMA expression than C57BL/6J mice (Fig. 3C). Immunostaining for NIMP-R4 demonstrated a lower number of polymorphonuclear neutrophils in the rTMD1 group compared to the PBS group on day 14, with $TM^{LeD/LeD}$ mice showing higher NIMP-R4 expression than C57BL/6J mice (Fig. 3D). Furthermore, TUNEL staining was applied to assess the cell-protective effect of rTMD1 on corneal alkali burns. An elevation in apoptotic cells was observed following the alkali burn, but the number of apoptotic cells significantly decreased in the rTMD1-treated group (Fig. 3E).

rTMD1 Attenuated the Expression of VEGF, VEGF-R1, TGF-β1, TNF-α, and CD86 and Increased CD206 Following Corneal Alkali Burn

In both C57BL/6J and $TM^{LeD/LeD}$ mice, the qRT-PCR results showed that the rTMD1-treated group exhibited suppression of VEGF, VEGF-R1, TGF-β1, and TNF-α, indicating the anti-angiogenesis, antifibrosis, and anti-inflammatory effects of rTMD1 (Figs. 4A–D). Additionally, there was a suppression of CD86 and an elevation of CD206 levels, suggesting a poten-

Investigative Ophthalmology & Visual Science

Downloaded from iovs.arvojournals.org on 01/10/2025

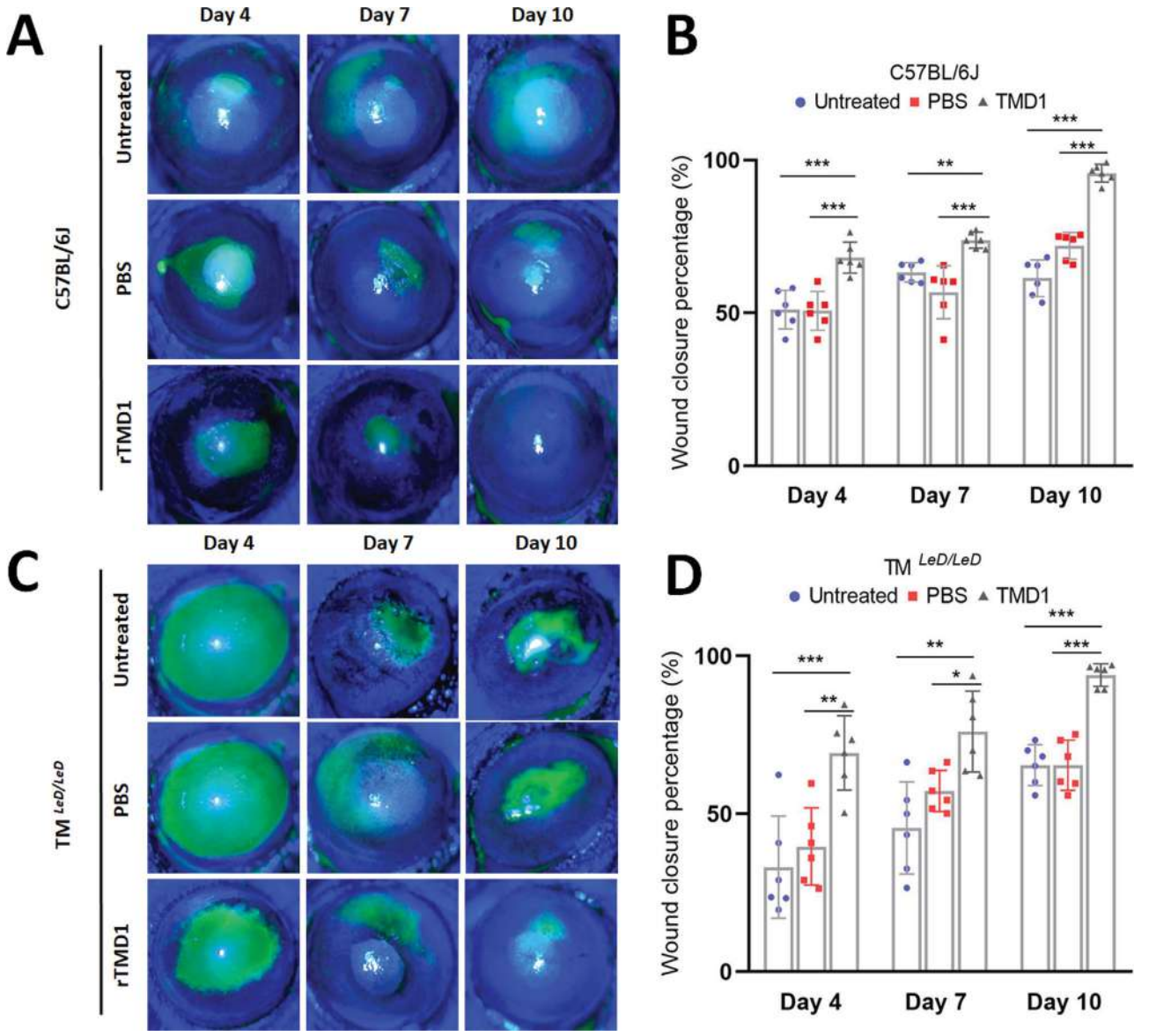


Figure 1. rTMD1 promotes corneal wound healing in both alkali burn–induced C57BL/6J and $TM^{LeD/LeD}$ mice. (**A**) Representative fluorescein-stained photographs of corneas. (**B**) Wound closure percentages on days 4, 7, and 10 in C57BL/6J mice. (**C**) Representative fluorescein-stained photographs of $TM^{LeD/LeD}$ mice corneas. (**D**) Wound closure percentages on days 4, 7, and 10. The data are expressed as mean ± SD (n = 6). *$P < 0.05$, **$P < 0.01$, ***$P < 0.001$, untreated versus PBS-treated versus rTMD1-treated.

tial association between rTMD1 and macrophage polarization (Figs. 4E, 4F).

rTMD1 Suppressed M1 Macrophage Polarization

To determine the effect of rTMD1 on macrophage polarization, THP-1 cells were treated with LPS and IFN-γ to induce an M1 macrophage phenotype. Cells were harvested 24 hours after rTMD1 incubation. The qRT-PCR results showed that rTMD1 administration led to a significant decrease in the expression of CD86 (Fig. 5A) and a concomitant increase in the expression of the M2 macrophage marker CD206 (Fig. 5B). Additionally, rTMD1 reduced ERK phosphorylation and HIF-1α expression in M1 macrophages, which may facilitate M2 polarization (Figs. 5C–E). These results indicate that rTMD1 promotes M2 polarization within an inflammatory microenvironment.

Discussion

Corneal chemical burns are severe ocular injuries that can lead to significant vision impairment or loss.[3] These injuries trigger acute inflammation, cellular damage, and tissue remodeling, often resulting in scarring and neovascularization.[22] Currently, corticosteroids are the primary treatment for managing inflammation induced by alkali burns to the cornea.[23] These potent anti-inflammatory drugs help to reduce the acute inflammatory response and prevent further damage.[23] However, their use comes with significant drawbacks. Corticosteroids can delay the wound healing process,

Investigative Ophthalmology & Visual Science

Downloaded from iovs.arvojournals.org on 01/10/2025

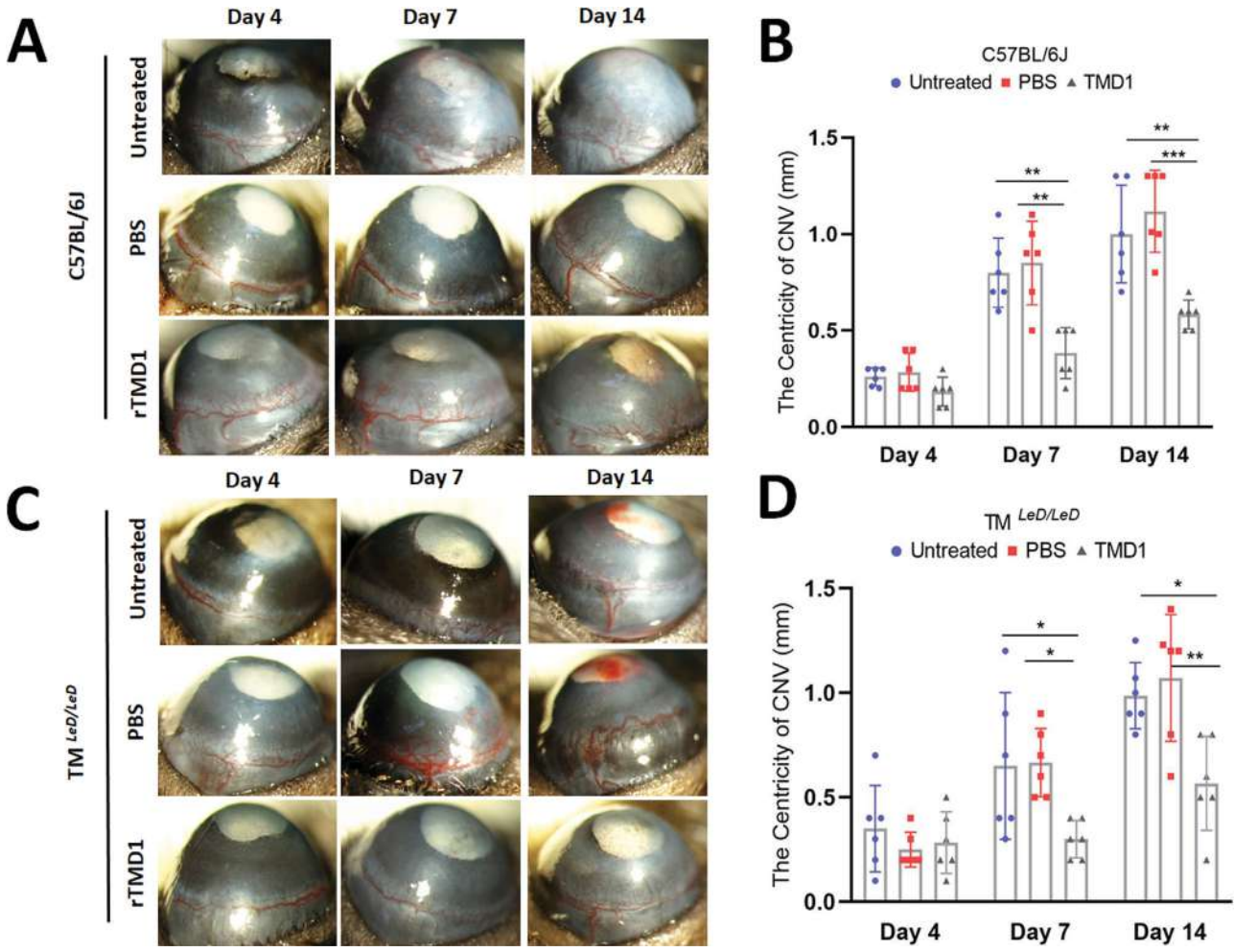


Figure 2. rTMD1 ameliorates CNV in C57BL/6J and TM$^{LeD/LeD}$ mice. (**A**, **B**) Representative CNV photographs of C57BL/6J mice corneas (**A**) and centricity of CNV (**B**) on days 4, 7, and 14. (**C**, **D**) Representative CNV photographs (**C**) and centricity of CNV (**D**) in TM$^{LeD/LeD}$ mice corneas on days 4, 7, and 14. The data are expressed as mean ± SD ($n = 6$). *$P < 0.05$, **$P < 0.01$, ***$P < 0.001$, untreated versus PBS-treated versus rTMD1-treated.

increase intraocular pressure, and elevate the risk of developing secondary infections due to their immunosuppressive effects.[23] Additionally, prolonged use of corticosteroids can lead to cataract formation and glaucoma, complicating long-term treatment strategies.[23] Anti-VEGF agents are another therapeutic approach, effectively inhibiting corneal neovascularization.[1] By targeting the VEGF pathways, these agents prevent the growth of new, abnormal blood vessels that can impair vision.[1] Despite their effectiveness, anti-VEGF therapies also have limitations. They can interfere with normal wound healing and regeneration processes, potentially leading to corneal thinning and other structural complications.[1,24,25] Given these challenges, there is an urgent need for new therapeutic agents that can effectively manage corneal inflammation and CNV without the adverse effects associated with current treatments. Innovations in drug development are focusing on agents that can modulate the inflammatory response more precisely and promote tissue repair, such as therapies targeting specific molecular pathways involved in inflammation and angiogenesis.

Our study demonstrates the therapeutic potential of rTMD1 in promoting corneal epithelial recovery, reducing neovascularization and corneal opacity, and mitigating inflammation and fibrosis following corneal alkali burn. In both C57BL/6J and TM$^{LeD/LeD}$ mice, rTMD1 significantly enhanced corneal epithelial healing at all observed time points, with notable improvements in wound closure rates compared to the PBS-treated group. rTMD1 treatment resulted in fewer and less tortuous blood vessels, as well as reduced corneal opacity, indicating its anti-angiogenic effects. Histological analysis has revealed that rTMD1 decreased corneal thickening and swelling, reduced polymorphonuclear neutrophil infiltration, and limited fibrosis, demonstrating its anti-inflammatory and antifibrotic properties. Additionally, rTMD1 protected corneal cells from apoptosis, as evidenced by fewer TUNEL-positive cells in treated groups. Molecular analysis further supported these findings, showing suppressed expression of VEGF, VEGF-R1, TGF-β1, and TNF-α, which are key mediators of angiogenesis, fibrosis, and inflammation. The modulation of macrophage polarization was also indicated by decreased CD86 and increased CD206 levels, suggesting that rTMD1 promotes a shift from pro-inflammatory M1 to reparative M2 macrophages. This shift is likely a crucial mechanism underlying the observed therapeutic effects.

Investigative Ophthalmology & Visual Science

Downloaded from iovs.arvojournals.org on 01/10/2025

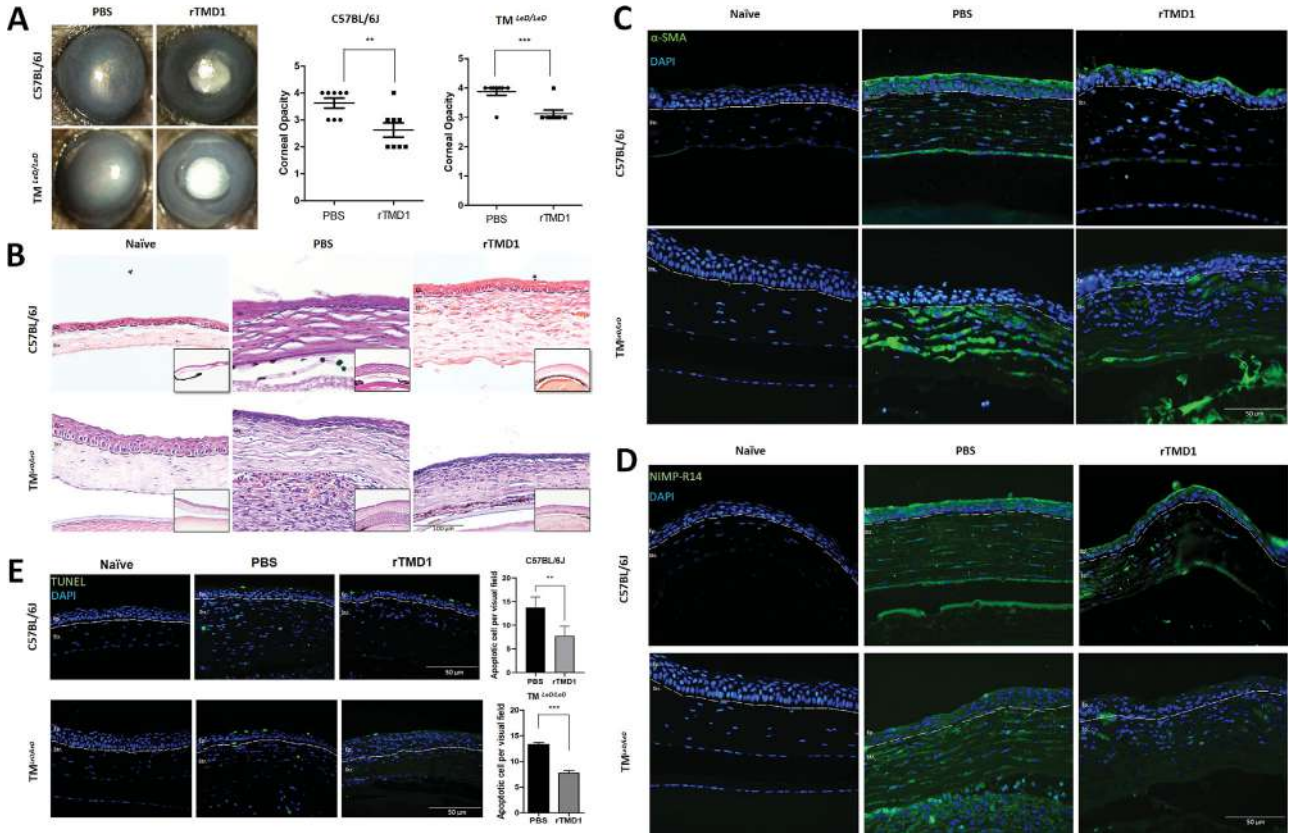


Figure 3. rTMD1 improves corneal opacity and exhibits antifibrosis, anti-inflammatory, and anti-apoptotic effects in *vivo*. (**A**) Corneal opacity of C57BL/6J and $TM^{LeD/LeD}$ mice in PBS- and rTMD1-treated groups on day 14. (**B**) Representative H&E staining of C57BL/6J and $TM^{LeD/LeD}$ mice on day 14 (magnification 400×, 50 µm). (**C**) α-SMA immunostaining of C57BL/6J and $TM^{LeD/LeD}$ mice in PBS- and rTMD1-treated groups on day 14. (**D**) NIMP-R4 immunostaining of C57BL/6J and $TM^{LeD/LeD}$ mice on day 14. (**E**) Representative images of TUNEL assay in C57BL/6J and $TM^{LeD/LeD}$ mice in each group on day 14 (magnification 400×, 50 µm). The data are expressed as mean ± SD ($n = 8$). $^{**}P < 0.01$, $^{***}P < 0.001$, PBS-treated versus rTMD1-treated.

Previous studies have demonstrated that angiogenesis, occurring under both physiological and pathological conditions, is closely linked to inflammation.[26] Inflammatory processes often accompany angiogenic events, contributing to the complexity of tissue responses. Soluble thrombomodulin (sTM) levels have been identified as a reliable biomarker reflecting endothelial damage and inflammation,[10] and they have been correlated with the clinical severity of various diseases, including cardiovascular disorders,[27,28] sepsis,[29] and diabetes.[30] These levels provide critical insights into the inflammatory status and the extent of endothelial injury in these conditions. rTMD1 has shown promising therapeutic potential in modulating inflammation. Conway et al.[18] first highlighted the significance of the lectin-like domain of thrombomodulin in inflammatory responses, noting that $TM^{LeD/LeD}$ mice exhibited exacerbated inflammatory reactions. Subsequent research revealed that rTMD1 could sequester high mobility group box B1 (HMGB1), a potent pro-inflammatory molecule, thereby mitigating inflammatory damage.[31] Additionally, rTMD1 was found to inhibit complement activation, further reducing inflammation.[32] We have discovered that inhibition of the HIF-1α pathway by rTMD1 could effectively rescue pathological angiogenesis in the retina.[33] This finding suggested a broader application for rTMD1, particularly in conditions characterized by excessive angiogenesis and inflammation, such as corneal alkali burn.

The initiation of CNV involves the release of pro-angiogenic factors, particularly VEGF, which stimulate the proliferation and migration of endothelial cells, leading to the formation of new capillaries.[34] Macrophages, key players in the immune response, significantly influence CNV through their polarization into M1 and M2 phenotypes.[35–37] M1 macrophages, activated by microbial products and pro-inflammatory cytokines, release high levels of pro-inflammatory mediators and reactive oxygen species, exacerbating tissue damage and promoting angiogenesis.[38] On the other hand, M2 macrophages, stimulated by anti-inflammatory signals, contribute to tissue repair and remodeling by producing anti-inflammatory cytokines and growth factors.[13] The dynamic balance between M1 and M2 macrophages is crucial; an imbalance can result in chronic inflammation, persistent CNV, and impaired corneal healing.[15,39,40] In our study, we observed significant changes in the polarization state of THP-1 cells upon treatment with rTMD1. Specifically, there was a marked decrease in the expression of the M1 macrophage marker CD86, which is commonly associated with pro-inflammatory responses. Concurrently, we noted an increase in the expression of the M2 macrophage marker CD206, indicative of an anti-inflammatory and tissue-repairing phenotype. This shift

Investigative Ophthalmology & Visual Science

Downloaded from iovs.arvojournals.org on 01/10/2025

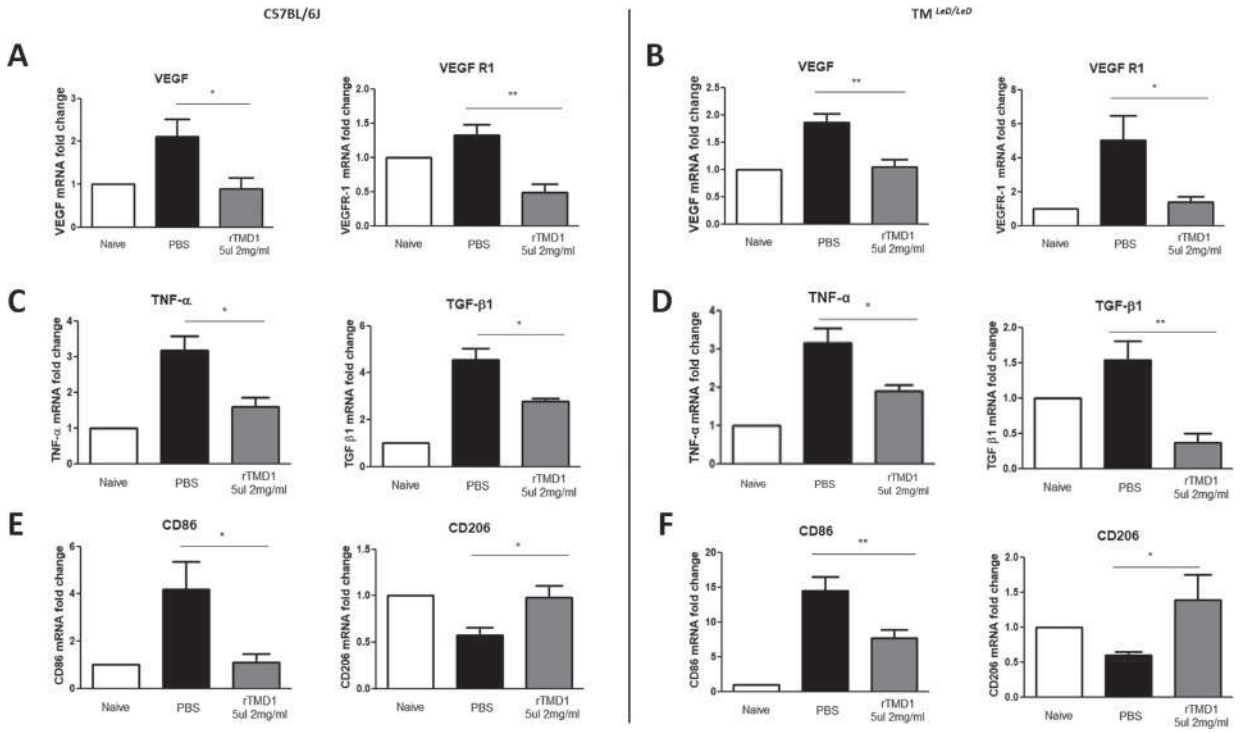


Figure 4. (**A**–**F**) rTMD1 reduced the expression of VEGF, VEGF R1, TNF-α, TGF-β1, and CD86 while increasing CD206 in the corneas of C57BL/6J and TM$^{LeD/LeD}$ mice with alkali-induced chemical burns on day 14. The data are presented as real-time PCR analysis of mRNA expression in day 14 corneas. Values are expressed as fold change relative to the control group. Data are expressed as mean ± SD ($n = 6$). *$P < 0.05$, **$P < 0.01$.

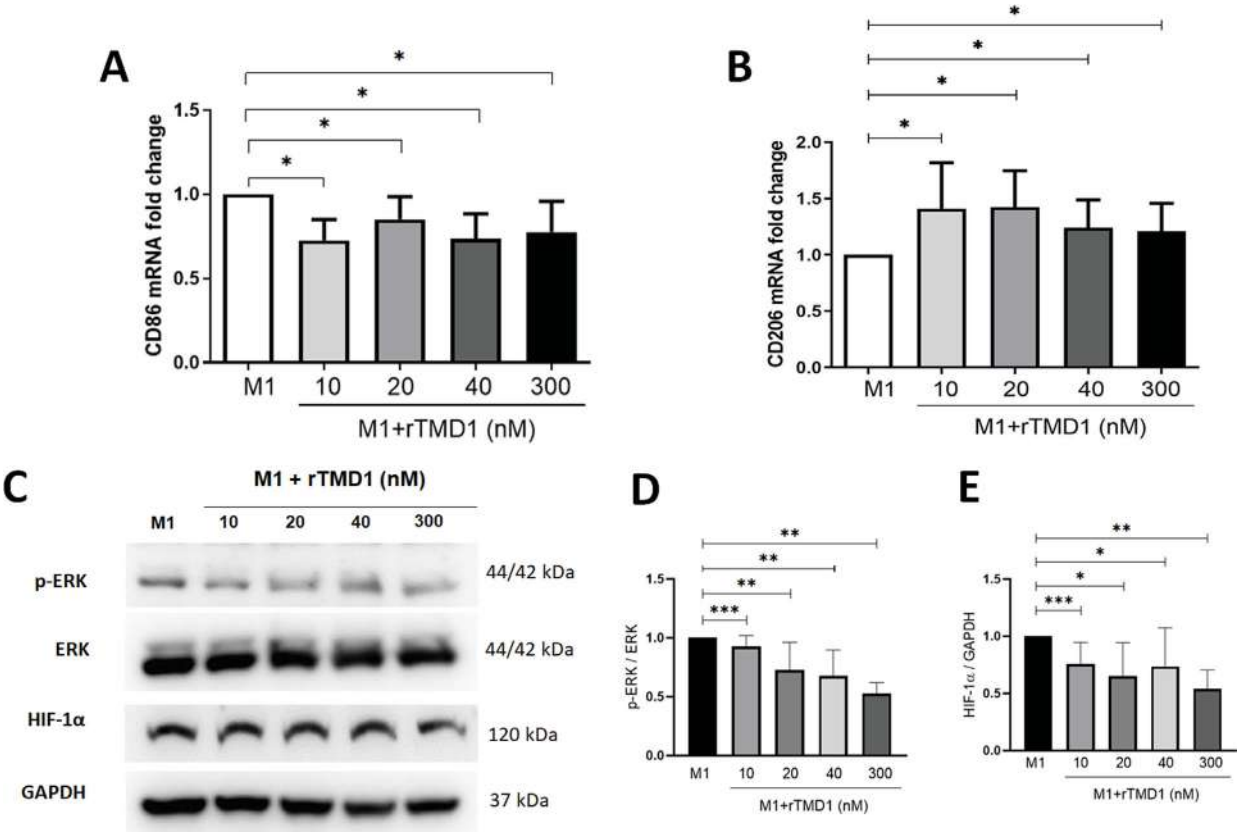


Figure 5. rTMD1 enhances M2 polarization by inhibiting the ERK/HIF-1α signaling pathway in rTMD1-treated M1 macrophages. (**A**, **B**) qRT-PCR data demonstrated that the addition of rTMD1 to the M1 induction medium disrupted M1 polarization (**A**) and enhanced polarization toward the M2 (**B**) phenotype. (**C**–**E**) Representative western blot results (**C**) and quantitative analysis of p-ERK/ERK (**D**) and HIF-1α/GAPDH (**E**) levels. Data are expressed as mean ± SD ($n = 3$). *$P < 0.05$, **$P < 0.01$, ***$P < 0.001$.

Investigative Ophthalmology & Visual Science

Downloaded from iovs.arvojournals.org on 01/10/2025

from M1 to M2 macrophages suggests that rTMD1 plays a pivotal role in modulating macrophage polarization, promoting a more reparative and less inflammatory cellular environment.

The ERK/HIF-1α pathway can influence macrophage polarization.[41] Hypoxia and HIF-1α have been shown to promote the M1 phenotype under certain conditions by enhancing the inflammatory response.[41] Conversely, the stabilization of HIF-1α can also contribute to M2 polarization in other contexts, particularly where tissue repair is required.[41] Our previous research revealed that rTMD1 plays a crucial role in inhibiting the HIF-1α/VEGF pathway, thereby mitigating pathological angiogenesis.[33] In our current study, we further substantiated these findings, demonstrating that rTMD1 consistently inhibits the ERK/HIF-1α pathway. This inhibition was evident in our experimental results, where we observed a significant reduction in HIF-1α stabilization and its transcriptional activity upon rTMD1 treatment. The suppression of ERK phosphorylation, a critical upstream activator of HIF-1α, further confirmed the efficacy of rTMD1 in modulating this signaling cascade.

rTMD1 plays a crucial role in modulating macrophage polarization, promoting the shift from a pro-inflammatory M1 phenotype to a reparative M2 phenotype.[17] This modulation is particularly beneficial in the context of corneal chemical burns, where excessive inflammation and neovascularization can lead to significant vision impairment. By enhancing M2 macrophage activity, rTMD1 helps to reduce inflammation, promote tissue repair, and control fibrosis, ultimately improving corneal healing and preserving vision. These properties make rTMD1 a promising candidate for therapeutic interventions in corneal injuries and other inflammatory conditions.

This study has several limitations, including its reliance on an animal model that may not fully reflect the complexity of human corneal injury and healing processes. Although the focus on macrophage polarization is important, this study does not investigate the potential effects of rTMD1 on other immune cells, such as neutrophils, or its influence on pro-inflammatory cytokines, which are crucial for inflammation and tissue repair after corneal chemical burns.[42] Additionally, rTMD1 may directly interact with tissue-resident cells, such as corneal keratinocytes and keratocytes, potentially enhancing epithelial and stromal regeneration. The precise molecular mechanisms underlying the effects of rTMD1, as well as its safety and efficacy in humans, remain to be determined. Future research should examine these mechanisms, optimize dosing strategies, investigate combination therapies, and evaluate long-term outcomes. Clinical trials will be essential to establish the therapeutic potential of rTMD1. If successful, rTMD1 could improve the management of corneal injuries and other inflammatory conditions by promoting healing, minimizing complications, and complementing existing treatments.

Conclusions

rTMD1 is a promising therapeutic agent for treating corneal chemical burns. Its multifaceted actions, including anti-inflammatory, cytoprotective, antifibrotic, and anti-angiogenesis effects, address the key pathological processes involved in corneal injury and healing. Our study, along with other preclinical studies, has shown encouraging results, paving the way for further research and potential clinical applications. With continued investigation, rTMD1 has the potential to significantly improve outcomes for patients suffering from corneal chemical burns, restoring vision and enhancing quality of life.

Acknowledgments

We thank Edward M. Conway (Centre for Blood Research, University of British Columbia, Vancouver, BC, Canada) for kindly providing the $TM^{LeD/LeD}$ mice.

Supported by a grant from the National Science and Technology Council (111-2314-B-006-072-MY3 to Y-HH).

Author Contributions: CHC and YHH involved in design and conduct of study. Collection and management of the data were done by CHC, ICP, and YHH. CHC, ICP, and YHH participated in management and interpretation of the data. CHC and YHH participated in preparation, review, and approval of the manuscript.

Disclosure: **C.-H. Chang**, None; **I.-C. Peng**, None; **Y.-H. Huang**, None

References

1. Sharma N, Kaur M, Agarwal T, Sangwan VS, Vajpayee RB. Treatment of acute ocular chemical burns. *Surv Ophthalmol*. 2018;63:214–235.
2. Wagoner MD. Chemical injuries of the eye: current concepts in pathophysiology and therapy. *Surv Ophthalmol*. 1997;41:275–313.
3. Eslani M, Baradaran-Rafii A, Movahedan A, Djalilian AR. The ocular surface chemical burns. *J Ophthalmol*. 2014;2014:196827.
4. Baradaran-Rafii A, Eslani M, Haq Z, Shirzadeh E, Huvard MJ, Djalilian AR. Current and upcoming therapies for ocular surface chemical injuries. *Ocul Surf*. 2017;15:48–64.
5. Bian F, Pelegrino FS, Henriksson JT, et al. Differential effects of dexamethasone and doxycycline on inflammation and MMP production in murine alkali-burned corneas associated with dry eye. *Ocul Surf*. 2016;14:242–254.
6. Rocha de Lossada C, Pagano L, Gadhvi KA, et al. Persistent loss of marginal corneal arcades after chemical injury. *Indian J Ophthalmol*. 2020;68:2543–2544.
7. Maruyama I, Bell CE, Majerus PW. Thrombomodulin is found on endothelium of arteries, veins, capillaries, and lymphatics, and on syncytiotrophoblast of human placenta. *J Cell Biol*. 1985;101:363–371.
8. Li YH, Kuo CH, Shi GY, Wu HL. The role of thrombomodulin lectin-like domain in inflammation. *J Biomed Sci*. 2012;19:34.
9. Conway EM. Thrombomodulin and its role in inflammation. *Semin Immunopathol*. 2012;34:107–125.
10. Kuo CH, Chen PK, Chang BI, et al. The recombinant lectin-like domain of thrombomodulin inhibits angiogenesis through interaction with Lewis Y antigen. *Blood*. 2012;119:1302–1313.
11. Lin WL, Chang CF, Shi CS, Shi GY, Wu HL. Recombinant lectin-like domain of thrombomodulin suppresses vascular inflammation by reducing leukocyte recruitment via interacting with Lewis Y on endothelial cells. *Arterioscler Thromb Vasc Biol*. 2013;33:2366–2373.
12. Biswas SK, Mantovani A. Macrophage plasticity and interaction with lymphocyte subsets: cancer as a paradigm. *Nat Immunol*. 2010;11:889–896.
13. Mosser DM, Edwards JP. Exploring the full spectrum of macrophage activation. *Nat Rev Immunol*. 2008;8:958–969.

Downloaded from iovs.arvojournals.org on 01/10/2025

14. Mantovani A, Sica A, Sozzani S, Allavena P, Vecchi A, Locati M. The chemokine system in diverse forms of macrophage activation and polarization. *Trends Immunol*. 2004;25:677–686.
15. Sica A, Mantovani A. Macrophage plasticity and polarization: in vivo veritas. *J Clin Invest*. 2012;122:787–795.
16. Wynn TA, Vannella KM. Macrophages in tissue repair, regeneration, and fibrosis. *Immunity*. 2016;44:450–462.
17. Huang TC, Wu HL, Chen SH, Wang YT, Wu CC. Thrombomodulin facilitates peripheral nerve regeneration through regulating M1/M2 switching. *J Neuroinflammation*. 2020;17:240.
18. Conway EM, Van de Wouwer M, Pollefeyt S, et al. The lectin-like domain of thrombomodulin confers protection from neutrophil-mediated tissue damage by suppressing adhesion molecule expression via nuclear factor κB and mitogen-activated protein kinase pathways. *J Exp Med*. 2002;196:565–577.
19. Bahar I, Kaiserman I, McAllum P, Rootman D, Slomovic A. Subconjunctival bevacizumab injection for corneal neovascularization. *Cornea*. 2008;27:142–147.
20. Yoon KC, Heo H, Kang IS, et al. Effect of topical cyclosporin A on herpetic stromal keratitis in a mouse model. *Cornea*. 2008;27:454–460.
21. Genin M, Clement F, Fattaccioli A, Raes M, Michiels C. M1 and M2 macrophages derived from THP-1 cells differentially modulate the response of cancer cells to etoposide. *BMC Cancer*. 2015;15:577.
22. Tuft SJ, Shortt AJ. Surgical rehabilitation following severe ocular burns. *Eye (Lond)*. 2009;23:1966–1971.
23. Singh P, Tyagi M, Kumar Y, Gupta K, Sharma P. Ocular chemical injuries and their management. *Oman J Ophthalmol*. 2013;6:83–86.
24. Kim TI, Chung JL, Hong JP, Min K, Seo KY, Kim EK. Bevacizumab application delays epithelial healing in rabbit cornea. *Invest Ophthalmol Vis Sci*. 2009;50:4653–4659.
25. Falavarjani KG, Nguyen QD. Adverse events and complications associated with intravitreal injection of anti-VEGF agents: a review of literature. *Eye (Lond)*. 2013;27:787–794.
26. Szade A, Grochot-Przeczek A, Florczyk U, Jozkowicz A, Dulak J. Cellular and molecular mechanisms of inflammation-induced angiogenesis. *IUBMB Life*. 2015;67:145–159.
27. Chan SH, Chen JH, Li YH, Lin LJ, Tsai LM. Increasing post-event plasma thrombomodulin level associates with worse outcome in survival of acute coronary syndrome. *Int J Cardiol*. 2006;111:280–285.
28. Ileri M, Hisar I, Yetkin E, et al. Increased levels of plasma thrombomodulin in patients with acute myocardial infarction who had thrombolytic therapy and achieved successful reperfusion. *Clin Cardiol*. 2001;24:377–379.
29. Iba T, Yagi Y, Kidokoro A, Fukunaga M, Fukunaga T. Increased plasma levels of soluble thrombomodulin in patients with sepsis and organ failure. *Surg Today*. 1995;25:585–590.
30. Thorand B, Baumert J, Herder C, Meisinger C, Koenig W. Soluble thrombomodulin as a predictor of type 2 diabetes: results from the MONICA/KORA Augsburg case-cohort study, 1984–1998. *Diabetologia*. 2007;50:545–548.
31. Abeyama K, Stern DM, Ito Y, et al. The N-terminal domain of thrombomodulin sequesters high-mobility group-B1 protein, a novel antiinflammatory mechanism. *J Clin Invest*. 2005;115:1267–1274.
32. Van de Wouwer M, Plaisance S, De Vriese A, et al. The lectin-like domain of thrombomodulin interferes with complement activation and protects against arthritis. *J Thromb Haemost*. 2006;4:1813–1824.
33. Huang YH, Kuo CH, Peng IC, et al. Recombinant thrombomodulin domain 1 rescues pathological angiogenesis by inhibition of HIF-1α-VEGF pathway. *Cell Mol Life Sci*. 2021;78:7681–7692.
34. Chang J-H, Gabison EE, Kato T, Azar DT. Corneal neovascularization. *Curr Opin Ophthalmol*. 2001;12:242–249.
35. Lu P, Li L, Mukaida N, Zhang X. Alkali-induced corneal neovascularization is independent of CXCR2-mediated neutrophil infiltration. *Cornea*. 2007;26:199–206.
36. Cursiefen C, Chen L, Borges LP, et al. VEGF-A stimulates lymphangiogenesis and hemangiogenesis in inflammatory neovascularization via macrophage recruitment. *J Clin Invest*. 2004;113:1040–1050.
37. Hadrian K, Willenborg S, Bock F, Cursiefen C, Eming SA, Hos D. Macrophage-mediated tissue vascularization: similarities and differences between cornea and skin. *Front Immunol*. 2021;12:667830.
38. Mantovani A, Sozzani S, Locati M, Allavena P, Sica A. Macrophage polarization: tumor-associated macrophages as a paradigm for polarized M2 mononuclear phagocytes. *Trends Immunol*. 2002;23:549–555.
39. Spiller KL, Anfang RR, Spiller KJ, et al. The role of macrophage phenotype in vascularization of tissue engineering scaffolds. *Biomaterials*. 2014;35:4477–4488.
40. Zhu Y, Tan W, Demetriades AM, et al. Interleukin-17A neutralization alleviated ocular neovascularization by promoting M2 and mitigating M1 macrophage polarization. *Immunology*. 2016;147:414–428.
41. Tang YY, Wang DC, Wang YQ, Huang AF, Xu WD. Emerging role of hypoxia-inducible factor-1α in inflammatory autoimmune diseases: a comprehensive review. *Front Immunol*. 2022;13:1073971.
42. Dua HS, Ting DSJ, Al Saadi A, Said DG. Chemical eye injury: pathophysiology, assessment and management. *Eye (Lond)*. 2020;34:2001–2019.

Investigative Ophthalmology & Visual Science

Downloaded from iovs.arvojournals.org on 01/10/2025